

# A near IR adaptive optics search for faint companions to early-type multiple stars<sup>\*</sup>

A.A. Tokovinin<sup>1</sup>, A. Chalabaev<sup>2</sup>, N.I. Shatsky<sup>1</sup>, and J.L. Beuzit<sup>3</sup>

<sup>1</sup> Sternberg Astronomical Institute, Universitetsky prosp. 13, 119899 Moscow, Russia (toko, kolja@sai.msu.su)

<sup>2</sup> Laboratoire d'Astrophysique, Observatoire de Grenoble, UMR5571, CNRS and Université J. Fourier, B.P. 53X, F-38041 Grenoble, France (chalabae@obs.ujf-grenoble.fr)

<sup>3</sup> Canada-France-Hawaii Telescope Corporation, P.O. Box 1597, Kamuela, HI 96743, USA (beuzit@cfht.hawaii.edu)

Received 22 January 1999 / Accepted 1 April 1999

**Abstract.** We report on a high dynamical range ( $> 10^m$ ) and high angular resolution (down to  $0.2''$ ) search for low-mass components of early-type primaries in 7 intermediate-age (5 Myr) multiple systems with the ESO 3.6 m telescope and the adaptive optics system ADONIS. The images were obtained in the  $J$  and  $SK$  bands with and without a coronagraphic mask of  $2''$  diameter. The census is nearly complete in the angular separation range  $1'' - 6''$ , corresponding to linear separations of 200–1200 AU, which have remained unstudied so far due to the intrinsic brightness of the massive primaries. The best detection limits are around  $K = 15^m$  at  $1''$  and  $K = 19^m$  at  $5''$  separation from the primary. In 13 fields of  $12.5'' \times 12.5''$  6 new faint stars were detected. Their magnitudes and colours indicate that 2 of them can be physical low-mass components. The bright ( $K = 11.2$ ,  $J - K = 1.2$ ) companion to HD 108250 C at  $2.17''$  has an IR excess and deserves further study. Several fields were explored without a mask; somewhat surprisingly, no new components at sub-arcsecond separations down to  $0.2''$  were detected. The first order stability analysis indicates that the studied multiple systems are hierarchical at spatial scales of 40–1000 AU. The data are briefly discussed in the light of the formation and evolution of multiple systems with massive primaries.

**Key words:** stars: binaries: close – stars: binaries: general – stars: early-type – stars: late-type – infrared: stars

## 1. Introduction

The formation mechanisms of binary and multiple stars constitute an important aspect of the general stellar formation process and are the subject of an active research. Observational work, providing unbiased statistics of periods and mass ratios, has first been carried out on low-mass binaries, both for the main sequence (Duquennoy & Mayor 1991, Tokovinin 1992) and the pre-main-sequence phases (Reipurth & Zinneker 1993, Prosser

et al. 1994, see also review by Mathieu 1994). But the knowledge of the multiple properties of massive stars is still highly incomplete due to the inherent observational difficulties.

The intrinsic brightness of massive stars demands imaging of very high dynamical range, about  $10^m$ , in order to detect faint low-mass companions; furthermore, high angular resolution is necessary since early-type stars are statistically at larger distances from the Sun than low-mass stars. The rarity of photospheric spectral lines limits the accuracy of radial velocity measurements. In spite of great efforts of observers in visible speckle-interferometry (Mason et al. 1998) and in radial velocity measurements (Brown & Verschueren 1997), the major physical properties of early-type multiple systems are known only for long periods and high mass ratios, biasing the statistics. Some additional information on low-mass components may be inferred from X-ray observations (Schmitt et al. 1993). However, the interpretation of data is often ambiguous (Berghöfer & Schmitt 1994, Berghöfer et al. 1997).

Progress in the technology of high sensitivity near-infrared array detectors yields changes in this situation. For example, the magnitude difference of a pair of B5V and M0V stars is considerably less at the longer wavelengths than at shorter wavelengths:  $10^m$  in  $V$ , and  $6^m$  in  $K$ . Thus, although limited to separations greater than  $1''$ , recent IR imaging provided first interesting clues. Young dense clusters rich in massive stars like the Orion Trapezium were shown to contain a population of low-mass pre-main-sequence stars (McCaughrean & Stauffer 1994). Herbig Ae/Be stars and FU Ori stars were shown to be surrounded by clusters of low-mass stars as well (Testi et al. 1997, Henning et al. 1998).

IR imaging combined with adaptive optics provides a new powerful tool to study the multiplicity of massive stars, tackling both the problem of high contrast and that of small separations. Indeed, the light of a faint companion is concentrated in the diffraction-limited core ( $0.12''$  at  $2.2 \mu$  with the 3.6 m telescope), while the background due to the light of the primary component is considerably reduced. With a coronagraphic mask the detection limit was pushed to a magnitude difference of  $\Delta K = 12.5$  at  $2''$  distance (Beuzit et al. 1997b). We report here on the observations of this kind applied for the first time to

Send offprint requests to: A. Tokovinin

<sup>\*</sup> Based on observations collected at the ESO La Silla Observatory (program 58.D-0455).

**Table 1.** List of observed stars

MSC	$\pi$ , mas	Age, Myr	HR	HD	Comp.	$V$	Sp. type		Sep., "	Sub-systems
06240-0658	4.7	4	2356	45725	A	4.60	B2Ve	AB	7.2	SB (12.5 <sup>y</sup> )?
			2357	45726	B	5.40	B2n	BC	2.8	
			2358	45727	C	6.20	B3Vne	CP	0.26	Visual
08065-4702	3.9	5	3207	68273	A	1.78	WC8+O9I	AB	41.2	SB2, 78.5 <sup>d</sup>
			3206	68243	B	4.27	B2III			SB1, 1.48 <sup>d</sup>
08226-3843	5.3	< 50	3327	71487	A	6.53	B9V	AB	8.1	Eclipsing, 1.257 <sup>d</sup>
			3328	71488	BC	7.25	A3V	BC	0.1	Visual binary
12210-6233	10.2	12	4730	108248	A	1.33	B0.5IV	AB	4.1	SB1, 75.8 <sup>d</sup>
			4729	108249	B	1.75	B1V			SB2
			4731	108250	C	4.86	B4V	AC	90	SB1, 1.225 <sup>d</sup>
15021-4454	8.0	15	5626	133955	AB	4.05	B3V	AB	0.4	Visual + SB?
15285-4050	5.8	< 50	5776	138690	AB	2.78	B2IV	AB	0.6	Visual + SB1, 2.8 <sup>d</sup>
15535-3807	6.6	5	5948	143118	A	3.41	B2.5IV	AB	15.0	SB?
			–	–	B	7.87	A5Vp			

the search of faint components in multiple systems with massive primaries.

For this first attempt, we selected systems as close as possible to the Sun. Another criterion of selection was the estimated age of stars. According to Sterzik & Durisen (1995), after formation of a cluster a fraction of low-mass stars should be ejected via dynamic interactions with more massive cluster members, producing extended coronae around star formation regions. The fraction of low-mass stars remaining after the cluster decay in gravitationally bound multiple systems with massive primaries is presently unknown, and it gives a strong constraint to understand the evolution. We address this question by selecting systems with ages of approximately 5 Myr, intermediate between young (Orion Trapezium, 1 Myr) and old (> 100 Myr) systems. By this time, the stars have already shed off most of the parental dust and gas so that the components should be easily detectable, having increased luminosity if they have not reached the Main Sequence yet.

The systems were selected from the Multiple Star Catalogue database (Tokovinin 1997, hereafter MSC). The spectral types of the primaries ranged from B0V to A0V. In the separation range of 0.2''–6'', only the massive visual components of the studied systems were previously known.

The programme systems are listed in Table 1. In the first 3 columns we give the MSC identifier for each system, the Hipparcos parallax (ESA 1997), and the age estimate from its association membership or nuclear evolution time. The separate visual components are identified by their HR and HD numbers and capital letters. Then follow visual magnitudes, spectral types, separations to the nearest visual companion, and comments on the closer sub-systems.

## 2. Observations and data reduction

We used the ESO 3.6 m telescope with the ADONIS adaptive optics system (Beuzit et al. 1997a) and the SHARP II camera

with a 256<sup>2</sup> NICMOS detector (Hofmann et al. 1992). In most cases, a coronagraphic mask of 2'' diameter (Beuzit et al. 1997b) was used to reduce the light from the primary. The observations were carried out on March 28 and 29, 1997, mainly in the  $J$  and  $SK$  bands with an image scale of 50 milliarcsec/pixel. The upper limit of the separation of detectable components is set by the field size of 12.8''  $\times$  12.8''. The minimum distance to the primary was set by the 1'' radius of the coronagraphic mask. For technical reasons the use of the fast shutter of the camera was impossible, so that unmasked imaging with diffraction-limited resolution of 0.12'' could be obtained only for the fainter primaries. To reduce further the light from the bright star, some exposures had to be taken through a narrow-band filter: a CVF at  $\lambda = 2.2 \mu$  and  $\lambda/\Delta\lambda = 60$  and a filter centered on the  $H_2$  line ( $\lambda = 2.121 \mu$ ;  $\Delta\lambda = 0.015 \mu$ ).

The data cube for each field consisted of a series of  $M$  object exposures, followed by a series of  $M$  sky/background exposures with an offset of about 15''. Exposure time ranged from 0.4 to 60 seconds, with  $M$  varying from 2 to 30. Series of flat field exposures were taken in the evening and in the morning using the sky of varying brightness as a source. The standard stars HR 3300 and HD 129655 were observed for photometric calibration. The seeing varied between 0.5'' and 1.2''.

Data were reduced using the Eclipse software package (Devillard 1997) specifically designed for adaptive optics image handling and processing and the ESO-MIDAS image analysis system. The data reduction included the usual steps of “bad” pixel intensity treatment (replacing it by the median value of adjacent pixels), sky background subtraction, and flat-fielding. Two techniques of flat field correction were tried: a “classical” flat field obtained as a median of normalized sky exposures and a flat field obtained by fitting the response of each detector pixel to the varying brightness of the dusk sky, as recommended in the Eclipse manual. The first method proved to yield better reproducibility and was adopted. The residual sensitivity variations

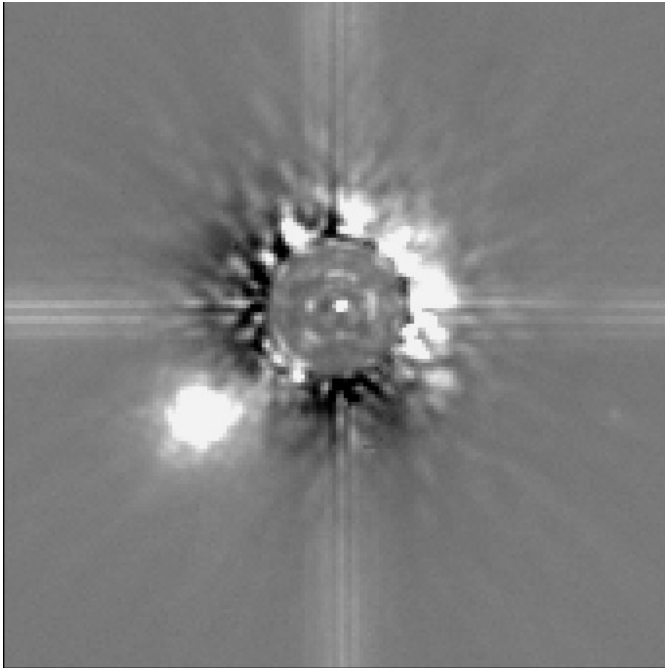


**Fig. 1.** Image of HD 108250 in the K band with a  $2''$  coronagraph mask. Only the central  $8.5'' \times 8.5''$  part is displayed, with North down and East to the left. The newly detected companion P ( $K = 11.2^m$ ) is seen in the lower left quadrant. The smooth radial component of the “wings” was subtracted, leaving a residual speckle structure and diffraction spikes. The asymmetry of the residual light is explained by the influence of P on our centering algorithm.

across the detector after flat field correction are estimated to be 2–3%.

The next step was to remove the “wings” of the bright star spilling around the coronagraph mask. First, the wing center was defined for each image (referred to hereafter as the image center). Then, the wing radial profile was constructed by computing the median intensity in annular zones versus the distance to the center. This smooth profile was subtracted, leaving high-frequency and ray-like features (Fig. 1). The faint sources could now easily be detected visually. However, we implemented an automated search scheme to get a reliable estimate of detection limits.

The detection limit in the vicinity of the primary is set by the residual halo which is dominated by a speckle-like pattern, especially in the  $K$  band. The phenomenon is well known for observations with adaptive optics both at ESO (Chalabaev et al. 1998) and at the CFHT (Walker et al. 1998, Racine et al. 1998). This “speckle” pattern is practically constant for frames of the same data cube but varies from source to source. We estimated the rms dispersion of the high-frequency variations,  $\sigma$ , of the residual intensity within the annular zones around the center of the primary image. The formal detection limit was set to  $3\sigma$ . In practice, an additional condition for the detection of faint sources was their presence in several frames.

For each image, the FWHM size of the Point Spread Function (PSF) was estimated (either from the images of bright com-

**Table 2.** Limiting magnitudes for the detection of components in coronagraphic images at various distances from the center

HD	Band	No CRN	Detection limits				
			1''	2''	3''	5''	
45725	A	K	–	12.5	14.6	16.1	17.0
			J	–	12.5	14.6	16.2
45726	B	K	+	14.0	15.0	14.7	16.7
			J	+	14.0	15.0	14.1
68273	A	K	–	10.0	11.7	13.2	14.4
			J	–	10.0	12.3	13.7
68243	B	K	+	12.5	14.7	15.8	16.8
			J	+	12.0	14.0	15.4
71487	A	K	+	15.0	17.4	18.2	18.8
			J	+	15.0	17.2	18.2
71488	BC	K	+	15.0	17.2	17.9	17.8
			J	+	14.0	16.0	16.9
108248	A	K	+	9.0	11.7	12.0	13.4
			J	–	9.0	10.9	11.5
108249	B	J	–	9.0	11.2	11.8	12.2
108250	C	K	–	13.5	14.3	16.9	17.6
			J	–	12.5	15.5	15.7
133955	AB	K	–	12.5	15.0	16.2	17.0
138690	AB	K	+	11.0	13.7	15.3	16.2
143118	A	K	–	10.5	13.3	14.6	15.5
			J	–	11.5	13.7	14.8
143118	B	K	+	15.0	17.0	17.2	17.4
			J	–	15.0	16.2	17.0

ponents without or outside mask, or by “guessing” from the speckles widths in the PSF wings). It enables us to establish an empirical relation between the source magnitude and the intensity in its central pixel, which is inversely proportional to the square of the FWHM. Using this relation and the photometric calibration, we converted the detection limits into magnitudes.

The  $3\sigma$  detection limits are given in Table 2 at distances of  $1''$ ,  $2''$ ,  $3''$ , and  $5''$  from the center. When a bright component was present outside the mask, the formally computed  $\sigma$  is wrong at a radius close to the component’s separation. In these instances, we give our best estimate of the true limits obtained by interpolation. The + sign indicates that images without mask have also been obtained and analyzed for the presence of components with separations from  $0.2''$  to  $1''$ . It is difficult to give quantitative detection limits in these cases. However, the procedure described above was successfully applied to several unmasked images. For example, for HD 68243 the detection limits at  $0.2''$  are  $7^m$  and  $8^m$  in  $J$  and  $K$  bands, respectively. They improve linearly up to a distance of  $2''$ , reaching  $13.3^m$  and  $14.7^m$ , and grow only slightly at greater distances from the center.

### 3. Results

Six new faint sources were detected in the 13 coronagraphic fields and none on the unmasked images. The magnitudes of the new objects were estimated by aperture photometry with a 16 pixel diameter and suitable subtraction of the adjacent background. Small corrections for atmospheric extinction were

**Table 3.** Positions, magnitudes, and colors of the new sources and photometry of the known components

I. New sources					
HD		$\rho$ , "	$\theta$ , deg.	$K$	$J - K$
68273	AP	4.72	13.3	13.40±0.08	0.75±0.09
71487	AP	5.44	264.6	17.34 0.10	2.44 0.50
108250	CP	2.17	52.4	11.21 0.03	1.24 0.06
108250	CQ	4.89	213.8	17.00 0.07	1.44 0.50
108250	CR	6.72	119.1	15.97 0.20	0.27 0.28
133955	AP	6.64	229.0	17.37 0.07	–
II. Known components					
HD		$K$	$J - K$		
45726	B	5.66	-0.12		
45727	C	5.34	0.19		
71487	A	6.95	-0.05		
71488	BC	6.99	0.07		

made, using values of  $0.10^m$  and  $0.08^m$  per air mass for the  $J$  and  $K$  bands. When sources were at the limit of detection in  $J$ , the color estimates are very crude. No color transformations were applied to our photometry. Its internal accuracy is about  $0.03^m$  for bright sources.

The separations and position angles of the new sources are determined relative to the image center. They are translated into arcseconds using the nominal pixel size of  $0.050''$  and assuming that detector rows are oriented in the East-West direction. We checked that the positions derived in this way for the two known binaries are in reasonable agreement with the catalogue values. The accuracy of our positional measurements was found to be better than 1 pixel as inferred from the internal agreement of the results.

With the limiting magnitudes around  $17^m$  in  $K$ , we would expect a considerable part of the faint objects detected to be background stars. Indeed, a source density of  $10^5$  per square degree would give one background object per  $12''$  field. The star count model of Ortiz & Lépine (1993) predicts such a star density near the Galactic equator already at  $K = 13.5^m$ , although the model predictions can only be used as an order-of-magnitude estimate as noted by Testi et al. (1997).

## 4. Discussion

### 4.1. Overview of the studied multiple systems

*HD 45725/26/27 =  $\beta^1$  Mon.* The 3 known bright components with comparable separations (trapezium) are certainly physical. They are all emission-line stars with fast rotation. The  $12^m$  component D at  $26''$  from A may also belong to the system. The magnitude difference between B and C is  $0.80^m$  in  $V$ , and only  $0.32^m$  in  $K$ . If the spectral types of B and C are indeed similar, the magnitude and color difference between B and C can be explained by differential absorption. On the basis of the combined

photometry of ABC it was claimed that this object shows an IR excess due to free-free emission (Dougherty et al. 1991). Our resolved photometry of BC will help to interpret the properties of this interesting and enigmatic system. The  $0.26''$  speckle pair CP = CHARA 167 was not detected on our unmasked images. Since its discovery in 1988 there were no confirming speckle measurements published.

*HD 68273/43 =  $\gamma^{2,1}$  Vel.* These young stars belong to the star formation region containing the Gum nebula. Its low-mass population was studied by Graham & Hege (1989). The visual components C, D, E at separations  $63'' - 93''$  from A are probably physical (Abt et al. 1976). No close visual components to A or B were discovered by speckle-interferometry (Mason et al. 1998). The new component P is likely to be physical. Its  $J - K$  colour and  $K$  magnitude correspond to a K4V dwarf slightly above the main sequence.

*HD 71487/88 = NO Pup.* A new source is found at  $5''$  from A. We suspect that it is a highly reddened ( $J - K = 2.4$ ) background star. In this region of sky there are other multiple systems with similar proper motions and radial velocities (e.g. HR 3283, 3322, 3359). Therefore, NO Pup belongs to an association.

*HD 108248/49/50 =  $\alpha^{1,2}$  Cru.* The coronagraphic images of C show a new bright component P ( $K = 11.2$ ) and at least two additional fainter components Q and R. While little can be said about the fainter sources, the P component is very likely physical, judging by its proximity to C and its brightness. Its colour  $J - K = 1.24$  is too red for a normal star, but not unusual for young low-mass T Tau stars as found in the compilation of Strom et al. (1989). This object may be similar to the “infrared companions” found in the vicinity of T Tau stars at comparable separations (see Mathieu 1994) with a very substantial difference that it accompanies a much brighter B-type primary. It is worth mentioning that several IR sources with  $K$  magnitudes up to 7.9 were discovered by Tapia (1981) within few arcminutes from the pair AB.

*HD 133955 =  $\lambda$  Lup.* A new source is discovered at a distance of  $5.6''$  from the close visual binary AB. No images with the  $J$  filter were taken and little can be said other than that the probability to find a background star of this magnitude is high.

*HD 138690 =  $\gamma$  Lup.* No new sources are found in the vicinity of this close visual binary.

*HD 143118 =  $\eta$  Lup.* As for the previous object, there are no new close companions found, but a ROSAT source at  $111''$  (Berghöfer et al. 1996) is likely to coincide with the known physical component C = HD 143099, a F5V dwarf at  $115''$  from AB.

### 4.2. Stability considerations

The typical distance to the systems is about 200 pc. Hence the largest measurable separation of  $6''$  corresponds to a size of 1200 AU. This gives the crossing time on the order of  $10^5$  yr, while the typical age of the programme systems is about  $5 \times 10^6$  yr. Therefore, one would expect that only quasi-stable hierarchical systems remain at the observed scale sizes. This assertion seems

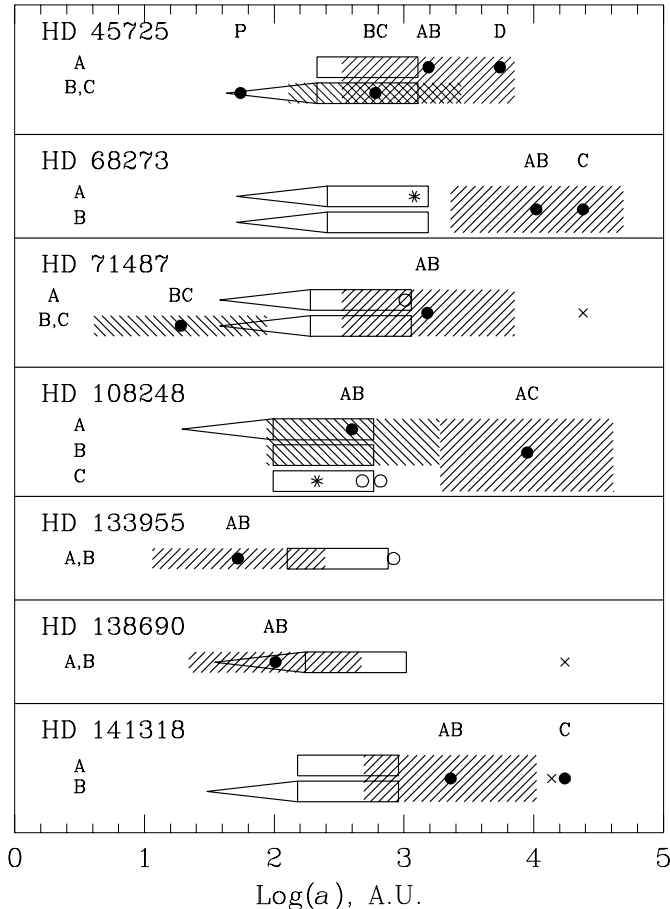


**Fig. 2.** Separation range surveyed by coronagraph is shown for each multiple system as a rectangle, with triangular extension to smaller separations when non-coronagraphic images were obtained. Known visible components are plotted as dots, with hatched areas indicating the separation range likely to be dynamically unstable. New components are indicated as asterisks (likely physical) and empty circles (likely optical), possible X-ray components (Berghöfer et al. 1996) are plotted as crosses.

to be verified by the data as discussed below. On the much larger scale of  $10^5$  AU ( $500''$ ), corresponding to a crossing time equal to the ages of the systems, one can naturally find unstable trapezium-type clusters similar to what was found around Ae/Be stars (Testi et al. 1997, Henning et al. 1998).

To obtain a first insight into the stability of the systems we will use an approximate criterion stating that triple systems with a ratio of outer period to inner period of more than 10 are stable. Known multiple stars seem to obey this simple rule (Tokovinin 1997), which translates into a ratio of the semi-major axes of  $10^{2/3} = 4.6$ . We make a further rough approximation by identifying the semi-major axis with the projected distance between the components,  $\rho$ . Thus, a pair of components with separation  $\rho$  is unlikely to have any inner sub-systems with separations more than  $\rho/4.6$ , and any distant components with separations less than  $4.6\rho$ .

In Fig. 2 we give a graphic representation of the surveyed separation range. Rectangles represent the  $1''$ – $6''$  range

with triangular extensions towards smaller separations if non-coronagraphic images were also available. Estimated instability zones are shown by hatching. For some systems the surveyed separations actually fall into these “instability shadows” cast by the known sub-systems, where no new components are to be expected. The presumably optical new companion to HD 71487 represents such a case.

The system HD 45725 A-BC may be on the edge of stability as far as can be judged by our approximate stability analysis. The component D is also likely to be unstable, as well as the components C, D, E of HD 68273. It is possible that both these medium-age systems are still in the chaotic phase of their dynamic evolution.

Examining Fig. 2, we note that two new companions that are likely to be physical are found well outside the instability zones. If they are indeed physical, the detection rate is  $2/5$ , because only 5 of the 13 surveyed coronagraphic fields are relatively free from instability constraints. The non-detection of new physical components in the remaining 8 “unstable” fields indicates that the medium-age multiple stars are indeed hierarchical at scales of  $300$ – $10^3$  AU.

Somewhat surprisingly, there are no detections in the smaller separation range from 40 to 300 AU, corresponding to observations of the 7 unmasked fields. Of course, the sensitivity limit was progressively worse for smaller separations (in fact, we missed the close companion of HD 45727). Still, we may speculate that the non-detections imply the real absence of low-mass companions in this range of distances. The distribution of the mass ratio would then depend on separation. An additional argument for this comes from Berghöfer et al. (1996), who observed in the X-rays all objects of our list except HD 68273. Only 3 systems were identified with RASS X-ray sources, but with offsets of  $\approx 100''$  (the maximum RASS positional error was estimated to be  $75''$ ).

Moving to small separations (below 0.1 AU), one finds spectroscopic binaries. Among the 4 single-lined spectroscopic binaries in our sample, 3 have orbits with low mass functions, implying the lower limits of secondary masses of 1.4, 1.0, and  $1.1 M_{\odot}$  for HD 68243, 108250, and 138690, respectively (cf. MSC). None of these low-mass companions was detected as an X-ray source. It is unlikely that these companions were formed so close to their primaries, but rather they were dragged into their actual short-period orbits via a dynamic interaction with the primaries or the circumstellar medium (cf. Gorti & Bhatt 1996). The same process may be responsible for removing companions at separations of 40–300 AU, while low-mass companions at larger separations survive. We must however note that better statistics is necessary to advance further with the theoretical analysis.

## 5. Conclusions

We reported on the first high dynamical range imaging search for low-mass companions of B-type stars at separations of  $0.2''$ – $6''$  ( $40$ – $10^3$  AU). Such performances became recently possible due to infrared imaging combined with adaptive optics and coronagraphy.

graphic masking. Among the 6 new faint sources, 2 are likely to be physical companions (to HD 68273 A and HD 108250 C), although further observations, in particular spectroscopy, are needed to confirm it and to identify component's nature.

So far, the presence of low-mass companions to massive stars has been reported from imaging observations of young clusters and fields around Herbig Ae/Be stars which were carried out with seeing limited angular resolution. The present work indicates that low-mass stars are also present in the intermediate-age (5 Myr) multiple systems with massive primaries in the separation range of several  $10^2$  AU. Surprisingly, no low-mass stars were detected at separations of 40–300 AU, while low-mass spectroscopic components at separations less than 0.1 AU are known to exist.

The systems examined here are found to be hierarchical at spatial scales of 40– $10^3$  AU. Additional observations of this kind must be conducted to build a firm statistical basis for the conclusions on the formation and evolution of multiple systems with massive primaries as sketched in this work. It is also necessary to extend the statistical studies of low-mass components to smaller separations of 0.1–40 AU with the help of long-baseline interferometers and spectroscopic and astrometric surveys of high precision.

*Acknowledgements.* The authors are grateful to the ESO La Silla 3.6 m telescope and the Infrared teams who prepared ADONIS and Sharp for these observations, and in particular to D. Le Mignant, J. Roucher, and U. Weilenmann. This project was initiated during the stay of A.T. at LAOG, Grenoble funded by the French Ministry of Education under the PAST contract. M. Schöck has kindly conceded to improve the English of our paper. The Simbad database operated at CDS, Strasbourg, France was used in this study.

## References

- Abt H.A., Landolt A.U., Levy S.G., et al., 1976, AJ 81, 541  
 Berghöfer T.W., Schmitt J.H.M.M., 1994, A&A 292, L5  
 Berghöfer T.W., Schmitt J.H.M.M., Cassinelli J.P., 1996, A&AS 118, 481  
 Berghöfer T.W., Schmitt J.H.M.M., Danner R., et al., 1997, A&A 322, 167  
 Beuzit J.-L., Demailly L., Gendron P., et al., 1997a, Exp. Astron. 7 285  
 Beuzit J.-L., Mouillet D., LARGANGE A.-M., et al., 1997b, A&AS 125, 175  
 Brown A.G.A., Verschueren W., 1997, A&A 319, 811  
 Chalabaev A., le Coarer E., Rabou P., et al., 1998, In: ESO/OSA Meeting on Astronomy with Adaptive Optics, Sonthoffen, Germany, 7–11 Sept. 1998, in print  
 Devillard N., 1997, Messenger 87, 17  
 Dougherty S.M., Taylor A.M., Clark T.A., et al., 1991, AJ 102, 1753  
 Duquenois A., Mayor M., 1991, A&A 248, 485  
 ESA, 1997, Hipparcos and Tycho Catalogues. ESA SP-1200  
 Gorti U., Bhatt H.C., 1996, MNRAS 283, 566  
 Graham J.A., Hege M.H., 1989, PASP 101, 573  
 Henning Th., Burkert A., Launhardt R., et al., 1998, A&A 336, 565  
 Hofmann R., Blietz M., Duboux P., et al., 1992, In: Ulrich M.H. (ed.) Progress in Telescope and Instrumentation Technologies. Proc. ESO 42, 687  
 Mason B.D., Gies D.R., Hartkopf W.I., et al., 1998, AJ 115, 821  
 Mathieu R.D., 1994, ARA&A 32, 465  
 McCaughrean M.J., Stauffer J.R., 1994, AJ 108, 1382  
 Ortiz R., Lépine R.D., 1993, A&A 279, 90  
 Prosser C., Stauffer J.R., Hartmann L., et al., 1994, ApJ 421, 517  
 Racine R., Walker G.A.H., Nadeau D., Doyon R., 1998, In: ESO/OSA Meeting on Astronomy with Adaptive Optics, Sonthoffen, Germany, 7–11 Sept. 1998, in print  
 Reipurth B., Zinnecker H., 1993, A&A 278, 81  
 Schmitt J.H.M.M., Zinnecker H., Cruddace R., et al., 1993, ApJ 402, L13  
 Sterzik M.F., Durisen R.H., 1995, A&A 304, L9  
 Strom K.A., Edwards S.E., Cabrit S., et al., 1989, AJ 97, 1451  
 Tapia M., 1981, MNRAS 197, 949  
 Testi L., Palla F., Prusti T., et al., 1997, A&A 320, 159  
 Tokovinin A., 1992, A&A 256, 121  
 Tokovinin A., 1997, A&AS 124, 75  
 Walker G., Chapman S., Mandushev G., et al., 1998, In: ESO/OSA Meeting on Astronomy with Adaptive Optics, Sonthoffen, Germany, 7–11 Sept. 1998, in print